Seismic site effects estimation from Probit analysis of the data of the 1976 Friuli earthquake (NE Italy)

S.Grimaz

Dipartimento di Georisorse e Territorio, Università degli Studi di Udine, Italy

(Received: August 27, 2008; accepted: January 23, 2009)

ABSTRACT After the earthquake of May 6, 1976 in Friuli (north-eastern Italy), a research team from the University of Udine (Italy) entered the data, compiled by specific technical groups immediately after the earthquake, on damage-inspection sheets, into a geo-located database. The database, named Fr.E.D. (Friuli Earthquake Damages), holds information on location, macroseismic intensity, construction typology and level of damage arising from the earthquake for each of the about 47,000 buildings. An "a posteriori" quantitative evaluation of local seismic response effects has been carried out using a Probit analysis of the data. In particular, relative amplification factors for some different geomorphological scenarios have been estimated.

1. Introduction

It is well known, and widely accepted in the community of earthquake engineers and seismologists, that surface geomorphology affects seismic motion and that those effects can be huge. Local amplifications have been shown as responsible for intensity variations as large as two degrees in the MM (Modified Mercalli) scale during the 1906 Great San Francisco earthquake, the 1985 Guerrero Michoacan earthquake in Mexico City, and the 1989 Loma Prieta event (Kramer, 1996).

Moreover, all recent destructive earthquakes (Spitak – Armenia 1988, Iran 1990, Philippines 1990, Northridge - California 1994, Kobe - Japan 1995, Armenia - Columbia 1999, Izmit - Turkey 1999, Bam - Iran 2003) have brought additional evidence of the dramatic importance of site effects.

Local amplification of ground motion due to site effects associated with subsurface geological settings were also observed in areas of moderate seismicity. Also, in smaller earthquakes, site effects can be responsible for the collapse of single buildings, as, for instance, in 2002 during the Molise (Italy) earthquake, when a single building (a school) collapsed, killing 30 children (Mucciarelli *et al*., 2003).

The fundamental phenomenon responsible for the ground motion amplification over soft sediments is the trapping of seismic waves due to impedance contrast (the product between seismic wave velocity and mean density) between sediments and underlying bedrock.

It has often been reported that, after destructive earthquakes, buildings located at hill tops suffered much more intensive damage than those located at the base. There is also clear instrumental evidence that surface topography has a considerable effect on the amplitude and frequency of ground motion (Géli *et al*., 1988; Faccioli, 1991; Finn, 1991). Theoretical and numerical models predict a systematic amplification of seismic motion at ridge crests, and, more

generally, over convex topographies such as cliffs. Correspondingly, they predict de-amplification over concave topographic features, such as valleys and at the base of hills (Pedersen *et al*., 1994). Other types of evidence have been shown and investigated in more recent studies (Martino *et al*., 2006; Wald and Allen, 2007; Laurenzano *et al*., 2008)

The number of instrumental studies on topographic effects is extremely low compared to studies dealing with layered soft soil amplification, and so more studies should be devoted to the topic of quantitative evaluation of the amplification effects of different geomorphologic scenarios (Di Bucci *et al*., 2005). The predictions derived from these studies must be tested and verified by comparison with actual macroseismic observations. On the other hand, it is possible to obtain "a posteriori" quantification of amplification for different geomorphological scenarios if statistical studies on damage levels observed in past earthquakes are feasable (Marzorati *et al.*, 2003).

In a recent study (Grimaz, 2009), a Probit analysis on the Friuli Earthquake Damage database was completed and Probit equations, which relate seismic action to the recorded damage for different typologies of buildings, were derived. For this study, a Probit analysis was applied for a quantitative evaluation of the differences in seismic action related to different levels of damage recorded for the same typology of buildings in different geomorphological scenarios.

2. Probit analysis

The Probit analysis was originally developed (Finney, 1971) for the analysis in biological and toxicological experiments where the response to some stimulus under study was 'quantal' or 'response or non-response' (e.g. death or survival, germinate or not germinate). Currently, these types of analyses have also been widely used in many other fields and, in particular, for risk assessment, where an adverse action affects a specific target (Lees, 1996; Vilchez *et al.*, 2001).

In every dose-response situation two components must be considered: the stimulus (for example a drug, a mental test, a physical force) and the subject (for example an animal, a plant, a human or a structure). If the characteristic response is quantal, occurrence or non-occurrence will depend upon the intensity of the stimulus (dose). For any one subject, there will be a certain level of intensity below which the response does not occur and above which the response occurs. This level is called tolerance and its value could vary from one subject to another of the population studied.

Therefore, a discussion of quantal response data requires recognition of the frequency distribution of tolerances over the population. The frequency distribution of tolerances, as measured on the natural scale can be converted into an approximate distribution of the familiar Gaussian or normal form (Fig. 1 graphic above). The transformed scale of doses where tolerances are normally distributed is known as metametric scale.

When stimulus is measured in metametric units, x, the curve of percentage responding against the dose takes the characteristic of a normal-sigmoidal form (Fig. 1 graphic in the middle). This curve approaches zero or 100% response at infinitely low and infinitely high values of dose.

On a transformed scale, a measure of probability of response is also possible, using the normal equivalent deviate (or N.E.D.). This response metameter is Y defined by Eq. (1):

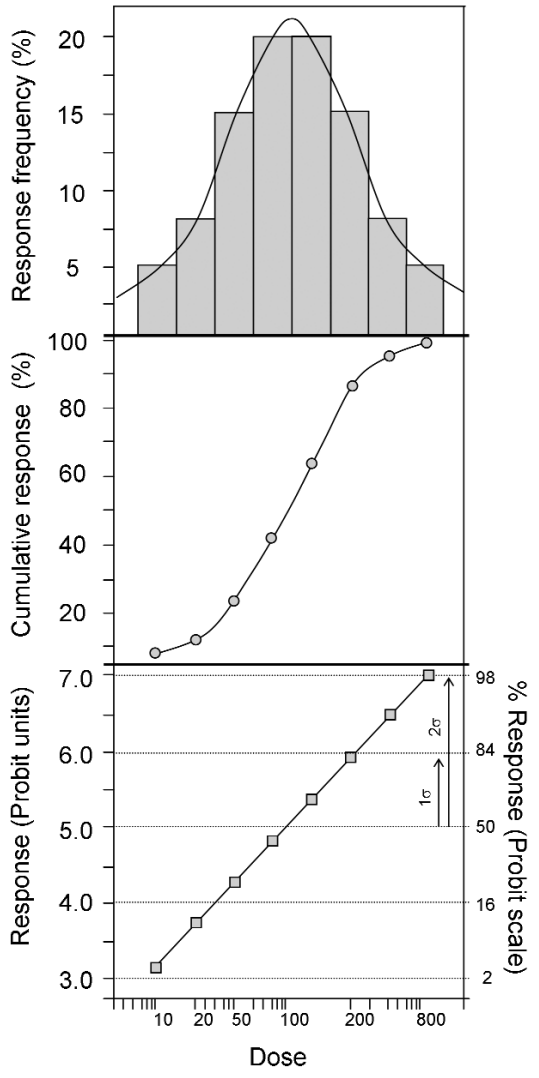

Fig. 1 - Diagram of quantal dose-response relationship [from Casarett (2001) modified].

$$P = \frac{1}{\sqrt{2\pi}} \int_{-\infty}^{Y} e^{-\frac{1}{2}u^2} du. \qquad (1)$$

Thus, the N.E.D. of any value of P between 0 and 1 is defined as the abscissa corresponding to the probability P in a normal distribution with mean 0 and variance 1.

After these transformations, the relation between the dose metameter, x, and the N.E.D. of the probability of response at that dose, is a straight line. In order to obtain only positive values, the Probit of P ("probit" = probability unit) is considered. For any P, the Probit, Y, is simply the N.E.D. increased by 5:

$$P = \frac{1}{\sqrt{2\pi}} \int_{-\infty}^{Y-5} e^{-\frac{1}{2}u^2} du. \qquad (2)$$

Also the relation between the Probit of expected proportion of responses and the dose is linear (Fig. 1 lowest part).

The linear equation is commonly defined as in Eq. (3):

$$Y = \alpha + \beta x \qquad (3)$$

where α, β, are derived by regression from experimental data, and x is the dose in the metametric scale.

Taking into account the fact that a typical frequency distribution for tolerance of a population, in a dose-response problem, is log-normal, the metametric scale can be obtained considering the logarithm of the dose [Eq. (4)]:

$$x = \log (V) \qquad (4)$$

where V is a measure of the intensity of the stimulus (or dose) and therefore represents the "causative variable".

The percentage response, observed for each dose, must first be calculated and converted to

Probit. The Probits are then plotted against the dose metameter, and a straight line can be obtained by linear regression.

Table 1 relates the Probit value Y to the percentage $P_{\%}$.

For computations, a more useful expression for the conversion from Probit to percentage is given by Eq. (5) (CCPS, 2000):

$$P_{\%} = 50\left[1 + \frac{Y-5}{|Y-5|} erf\left(\frac{|Y-5|}{\sqrt{2}}\right)\right]. \tag{5}$$

If it is possible to obtain $P_{\%}$ from observation; it is also possible to derive the associated Probit Y value and then relate the causative variable V to the observed percentage of the specific level of response of the affected target.

An inverse relationship could also be derived as in Eq. (6):

$$\log V = a + bX_{probit} \tag{6}$$

where a and b are obtained by regression from experimental data, $\log V$ is the dose in the metametric scale and X_{probit} is the Probit corresponding to the observed percentage $P_{\%}$.

This method, widely applied in the field of risk assessment of major accidents, biology and toxicology, can also be applied to seismic risk assessment in order to evaluate vulnerability curves. In this case, the parameter V is considered as an indicator of the severity of the action (for example, referring to accelerometric measures), and the specific damage level recorded as the response.

Table 1 - Relationships between Probit value Y (in italic) and percentage $P_{\%}$.

$P_{\%}$		units									
		0	**1**	**2**	**3**	**4**	**5**	**6**	**7**	**8**	**9**
tens	**0**	-	*2.67*	*2.95*	*3.12*	*3.25*	*3.36*	*3.45*	*3.52*	*3.59*	*3.66*
	10	*3.72*	*3.77*	*3.82*	*3.87*	*3.92*	*3.96*	*4.01*	*4.05*	*4.08*	*4.12*
	20	*4.16*	*4.19*	*4.23*	*4.26*	*4.29*	*4.33*	*4.36*	*4.39*	*4.42*	*4.45*
	30	*4.48*	*4.50*	*4.53*	*4.56*	*4.59*	*4.61*	*4.64*	*4.67*	*4.69*	*4.72*
	40	*4.75*	*4.77*	*4.80*	*4.82*	*4.85*	*4.87*	*4.90*	*4.92*	*4.95*	*4.97*
	50	*5.00*	*5.03*	*5.05*	*5.08*	*5.10*	*5.13*	*5.15*	*5.18*	*5.20*	*5.23*
	60	*5.25*	*5.28*	*5.31*	*5.33*	*5.36*	*5.39*	*5.41*	*5.44*	*5.47*	*5.50*
	70	*5.52*	*5.55*	*5.58*	*5.61*	*5.64*	*5.67*	*5.71*	*5.74*	*5.77*	*5.81*
	80	*5.84*	*5.88*	*5.92*	*5.95*	*5.99*	*6.04*	*6.08*	*6.13*	*6.18*	*6.23*
	90	*6.28*	*6.34*	*6.41*	*6.48*	*6.55*	*6.64*	*6.75*	*6.88*	*7.05*	*7.33*

If the information, on the response of many typologies of buildings with different behaviours under the same seismic load is complete, it is possible to consider them as different subjects and carry out a separate Probit analysis for each typology of building (i.e. classified in the same vulnerability class) obtaining, for each of them, the relative Probit relationships (Grimaz, 2009). Alternatively, if we refer to a set of buildings belonging to the same vulnerability class, it is possible to define the level of dose (seismic action) causing a specific grade of damage. Hence, the Probit analysis can be also used as a tool for quantitative measures of the local effect in terms of ground motion amplification in correspondence with different geomorphologic scenarios.

3. The Friuli Earthquake Damage database

After the May 6, 1976 earthquake in Friuli (north-eastern Italy), about 85,000 damaged buildings were inspected as required by a subsequent regional law (LR. 17/76 - Friuli Venezia Giulia Region), and the same number of survey forms was completed and collected. The aim of that survey was to define the number of dwellings that were not usable after the earthquake and to assess the cost of repairing them. The data set contained information on the damage level caused to the building and on the characteristics of the building.

Studies made immediately after the earthquake (Giorgetti, 1976) produced an assessment of the isoseismal curves for the event for the whole region affected by the earthquake.

At the beginning of 1990, a research team of the University of Udine acquired all the sheets collected in 1976, and organized them in a database (Friuli Earthquake Damages – Fr.E.D.). Studies on seismic vulnerability were carried out (Grimaz, 1993; Grimaz *et al*., 1997). Riuscetti *et al*. (1997) and Carniel *et al*. (2001), in particular, used Fr.E.D. data and defined six, meaningfully different, classes of vulnerability corresponding to six different typologies of buildings (see Table 2).

Table 2 - Vulnerability typologies with statistically different outcomes in the Fr.E.D. database.

Building characteristics					**Vulnerability Typology**
Material		Construction date	Structural context	floor	
masonry	stone	< 1920	detached building or not detached buildings	< 5	T1
		1920-1950	detached building or not detached buildings	3-5 < 5	T2
		1920-1950	detached building	1-2	T3
	stone/bricks	>1950	detached building or not detached buildings	3-5	T4
		>1950	not detached building	1-2	T5
		>1950	detached building	1-2	T6

By using other information present in the sheets, for example the address (which identifies the location of each building), the data were geo-localized and an automatic evaluation of the typology and seismic intensity experienced at the site of each building was defined. The result was a new release of the Fr.E.D. database in which a set of about 47,000 buildings with localization, causative variable, class of vulnerability and relative damage provoked were reconstructed. The numbers of buildings belonging to the different vulnerability typologies of the Fr.E.D. database are shown in Fig. 2.

The Fr.E.D. damage classification was compared with the EMS98 (Grünthal, 1998) damage scale as shown in Table 3 and the damage of the buildings can be expressed by EMS98 scale.

A new sub-grade (G5+) has been introduced to distinguish the upper part of grade G5 of the EMS98 scale, corresponding to the complete destruction of a building (this distinction is present in the Fr.E.D. damage classification).

The information contained in the new release of the Fr.E.D. database enables us to use the Probit analysis to derive "a posteriori" quantification of the ground motion amplification for different geomorphologic scenarios.

In order to define dichotomous values of damage and develop the Probit analysis, threshold limits have been defined, and the corresponding ranges have been used in the Probit analysis (see Table 4).

4. Ground motion variables

The majority of buildings in the Fr.E.D. database are masonry constructions. The damage to this type of building, considering their hysteretic behaviour, is better related to the energy of ground shaking, and therefore also to the peak ground velocity (PGV). On the other hand, hazard maps generally forecast the severity of ground motion in terms of peak ground acceleration (PGA). Therefore, both PGA and PGV have been considered as causative variables in the

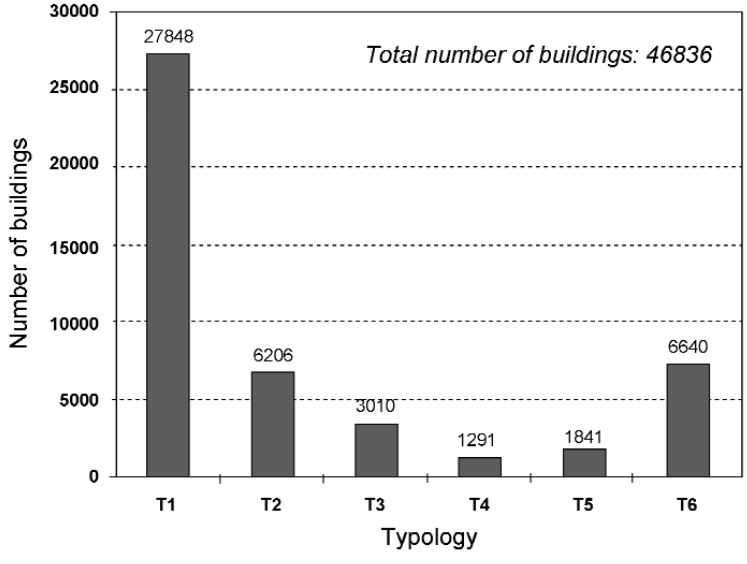

Fig. 2 - Distribution of different vulnerability typologies in the Fr.E.D. database.

Table 3 - Correspondence between EMS98 grade and FrED damage level (Grimaz *et al*., 1996).

EMS98	**≤G3**	**G4**	**G5**	**G5⁺**
FrED	TR	PR	NR	D
TR = totally recoverable PR = partially recoverable NR = not recoverable D = destroyed				

investigations.

In the case of the 1976 Friuli earthquake, the ground motion parameters have been derived "ex-post" from macroseismic intensity using empirical relationships. In particular, Faccioli and Cauzzi's (2006) relationships have been used. Faccioli and Cauzzi (2006) analysed data from several earthquakes in the Mediterranean area and obtained relationships between macroseismic intensity I and maximum acceleration (a_{max}) and between I and maximum velocity (v_{max}).

In their investigations, they used the acceptable approximation that $I = I_{MCS} = I_{MSK}$ and obtained the following relationships:

$$I = (6.54 \pm 0.10) + (1.96 \pm 0.29) \log a_{\max} \qquad R^2 = 0.38 \tag{7a}$$

$$I = (8.69 \pm 0.22) + (1.80 \pm 0.17) \log v_{\max} \qquad R^2 = 0.61. \tag{7b}$$

The relationships are valid for the range of $4/5 \leq I \leq 9$.

Using the same set of data from which Faccioli and Cauzzi (2006) derived Eqs. (7a) and (7b), Eqs. (8a) and (8b), with $\log(a_{max})$ and $\log(v_{max})$ as dependent variables and I as an independent variable, have been derived here:

$$\log a_{\max} = (0.2 \pm 0.03) I - (1.33 \pm 0.19) \qquad R^2 = 0.38 \tag{8a}$$

$$\log v_{\max} = (0.35 \pm 0.03) I - (3.53 \pm 0.21) \qquad R^2 = 0.61. \tag{8b}$$

Eqs. (8a) and (8b) are valid in the range of $4/5 \leq I \leq 9$ and assume $I = I_{MCS} = I_{MSK}$. Eqs. (8a) and (8b) can be used to define, "ex-post", respectively the average peak acceleration and the average

Table 4 - Ranges of damage considered in the Probit analysis.

FrED	TR-D	PR-D	NR-D	D
EMS98	**≥G3**	**≥G4**	**≥G5**	**G5⁺**

peak velocity of the ground motion considering the macroseismic intensity as independent variable.

5. Regional inverse Probit curves

The average values of PGA and PGV, derived using Eqs. (8a) and (8b), have been used as causative variable (V) in the Probit analysis.

Considering the Probit value as an independent variable (this is why X_{probit} is used instead of Y) and $\log(a_{max})$ and $\log(v_{max})$ as dependent variables, the Probit curves of the inverse relationship (response-dose instead of dose-response) have been derived from the whole regional area (these curves are called "inverse Probit" in this work). Table 5 shows the data utilised for the Probit analysis applied on the most representative typology of buildings, T1 (this is because this typology is present in all of the regional territory).

T1 buildings suffering a damage of $\geq G5$ and $\geq G4$ have been considered in the analysis and inverse Probit curves have been derived in terms both of a_{max} and v_{max}.

The following regional inverse curves of Probit were obtained:

$$\log a_{\max} = (0.25 \pm 0.04) X_{probit|T1 \geq G5} - (0.73 \pm 0.16) \quad R^2 = 0.89 \tag{9a}$$

$$\log a_{\max} = (0.26 \pm 0.04) X_{probit|T1 \geq G4} - (0.69 \pm 0.16) \quad R^2 = 0.88 \tag{9b}$$

$$\log v_{\max} = (0.46 \pm 0.07) X_{probit|T1 \geq G5} - (2.48 \pm 0.29) \quad R^2 = 0.89 \tag{10a}$$

$$\log v_{\max} = (0.44 \pm 0.07) X_{probit|T1 \geq G4} - (2.41 \pm 0.28) \quad R^2 = 0.88 \tag{10b}$$

Fig. 3 illustrates the linear regression curves with the 95% confidence interval of the mean

Table 5 - Regional data utilized for the inverse curve of the Probit estimation.

I_{MSK}	$\log(a_{max})$	$\log(v_{max})$	Total buildings T1	Buildings damaged ≥G5	%	$X_{probit\|\geq G5}$	Buildings damaged ≥G4	%	$X_{probit\|\geq G4}$
VI-VII	-0.03	-1.26	3567	24	0.7	2.54	49	1.4	2.80
VII	0.07	-1.08	5861	91	1.6	2.85	204	3.5	3.19
VII-VIII	0.17	-0.91	5715	162	2.8	3.09	306	5.4	3.39
VIII	0.27	-0.73	8088	1257	15.5	3.99	1873	23.2	4.27
VIII-IX	0.37	-0.56	1921	570	29.7	4.47	834	43.4	4.83
IX	0.47	-0.38	1537	394	25.6	4.34	654	42.6	4.81
X	0.67	-0.03	789	294	37.3	4.68	404	51.2	5.03

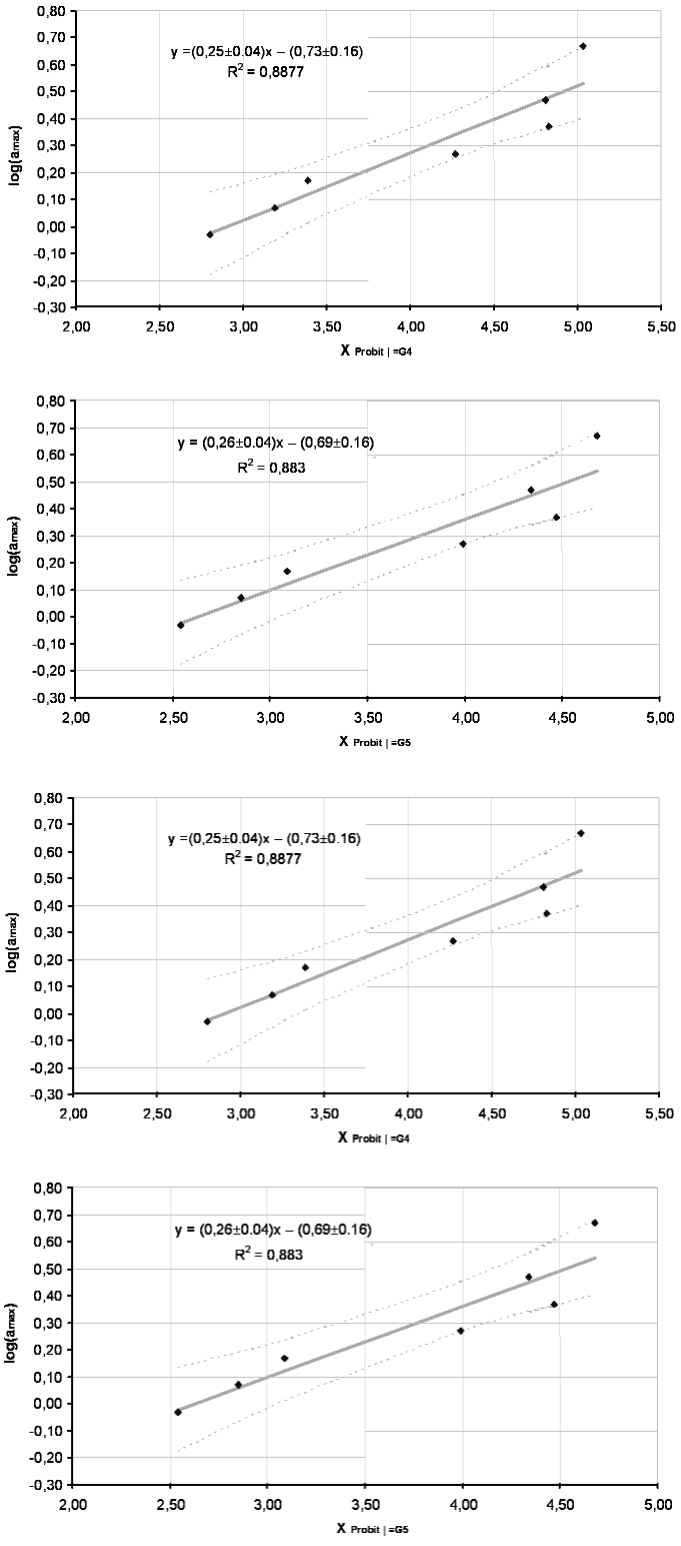

Fig. 3 - Regional inverse curves of Probit derived from T1 buildings in the Fr.E.D. database.

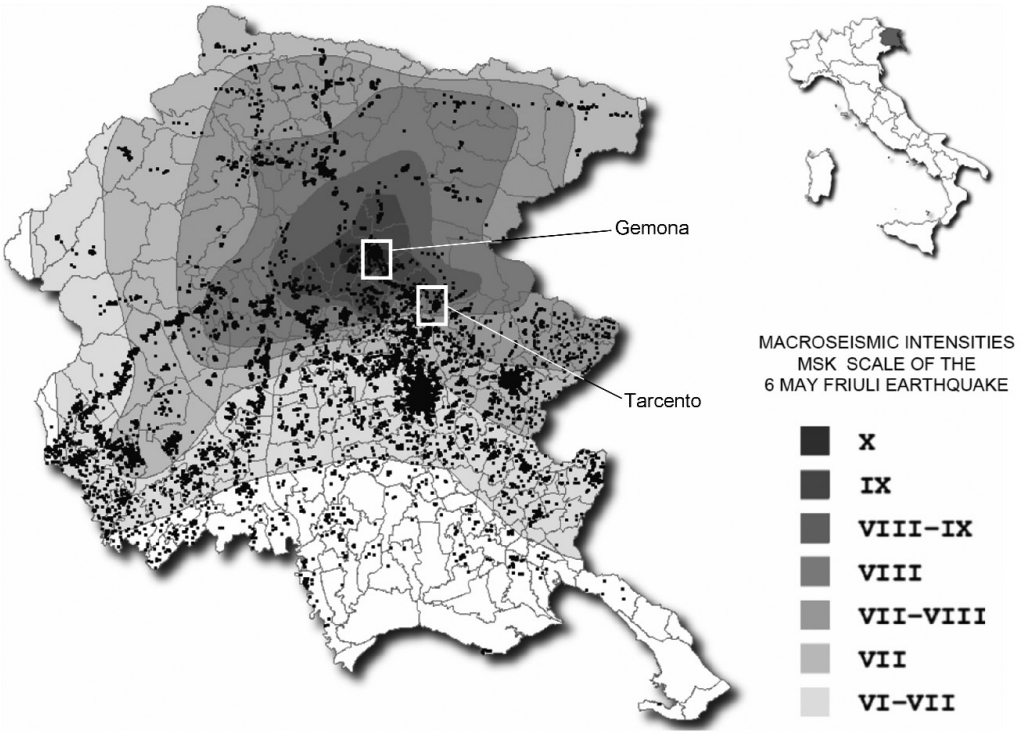

Fig. 4 - Localization of areas of study at Gemona and Tarcento (the dots represent the buildings in the Fr.E.D. database).

response. The confidence interval has been calculated with n-2 degrees of freedom, where n=7 is the size of the original data set (grades of I_{MSK} considered).

6. Quantification of different ground motions for different geomorphologic scenarios

The inverse Probit relationships derived above allow us to relate the damage to the ground motion parameter which can be considered as causative variable for that level of damage.

Two areas were considered as study sites: Gemona and Tarcento (indicated in Fig. 4).

They were chosen because each area presents different, adjacent geomorphologic features that can be considered at the same epicentral distance. Therefore, different damage on buildings belonging to the same vulnerability class must be related to site effects only.

In both areas of study, for each different geo-morphotypes there is a sufficient number of damaged buildings of the same typology T1, therefore, the inverse Probit relationships used to obtain an estimation of the ground motion, in terms of a_{max} and v_{max}, from the damage observed in the different geo-morphotypes, can be applied with reference to that typology of buildings.

Within the areas of study, the geomorphologic scenarios have been classified, taking also into account the indications of Eurocode 8 (CEN, 2004) as the "geo-morphotypes" illustrated in Fig. 5.

Inverse Probit equations were applied to the different geo-morphotypes of the two areas

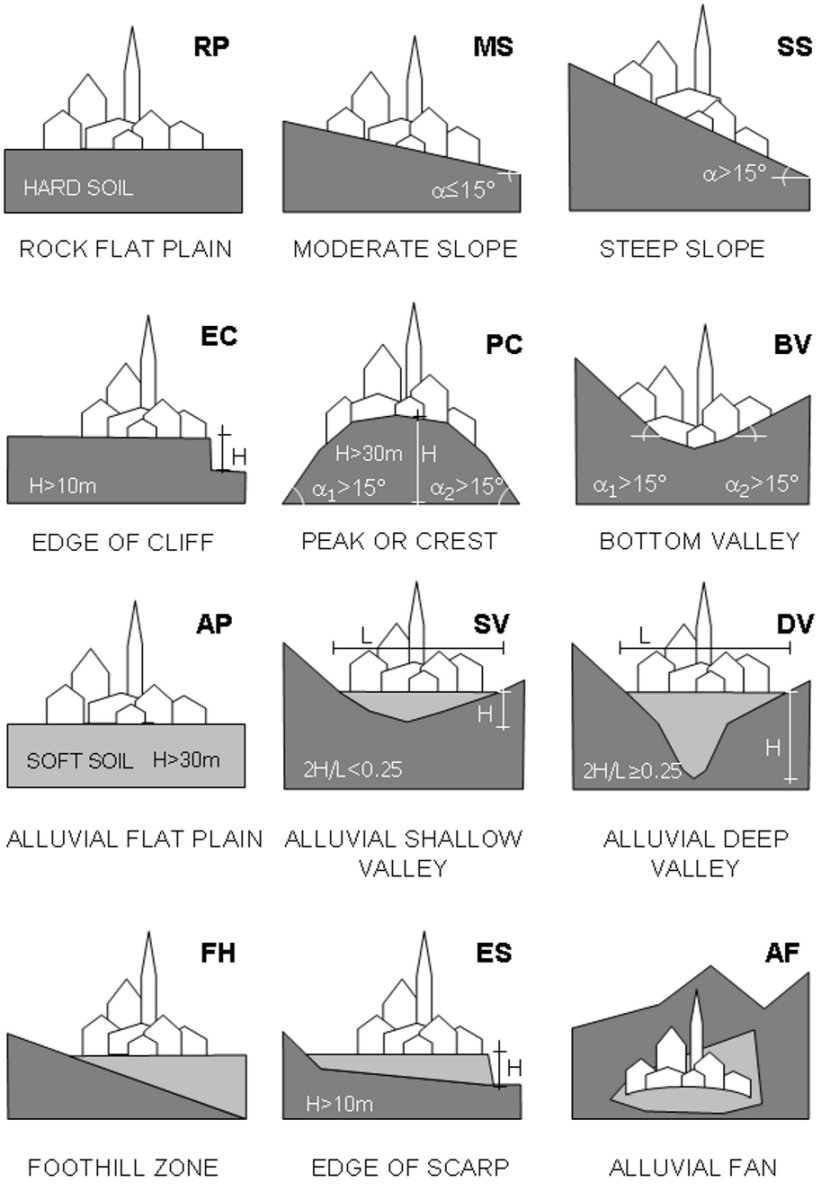

Fig. 5 - Classification of geo-morphotypes according to Eurocode 8.

and both a_{max} and v_{max} values were calculated (Tables 6 and 7 and Fig. 8). The geo-morphotype flat plane was considered as a reference geo-morphotype and the amplification of other geo-morphotypes was expressed as a ratio with respect to that flat plain geo-morphotype.

The average relative amplification factors referred to the alluvial flat plane geo-morphotype have been derived and are shown in Tables 6 and 7.

The results of the Probit analysis for Gemona and Tarcento are shown in Fig. 8.

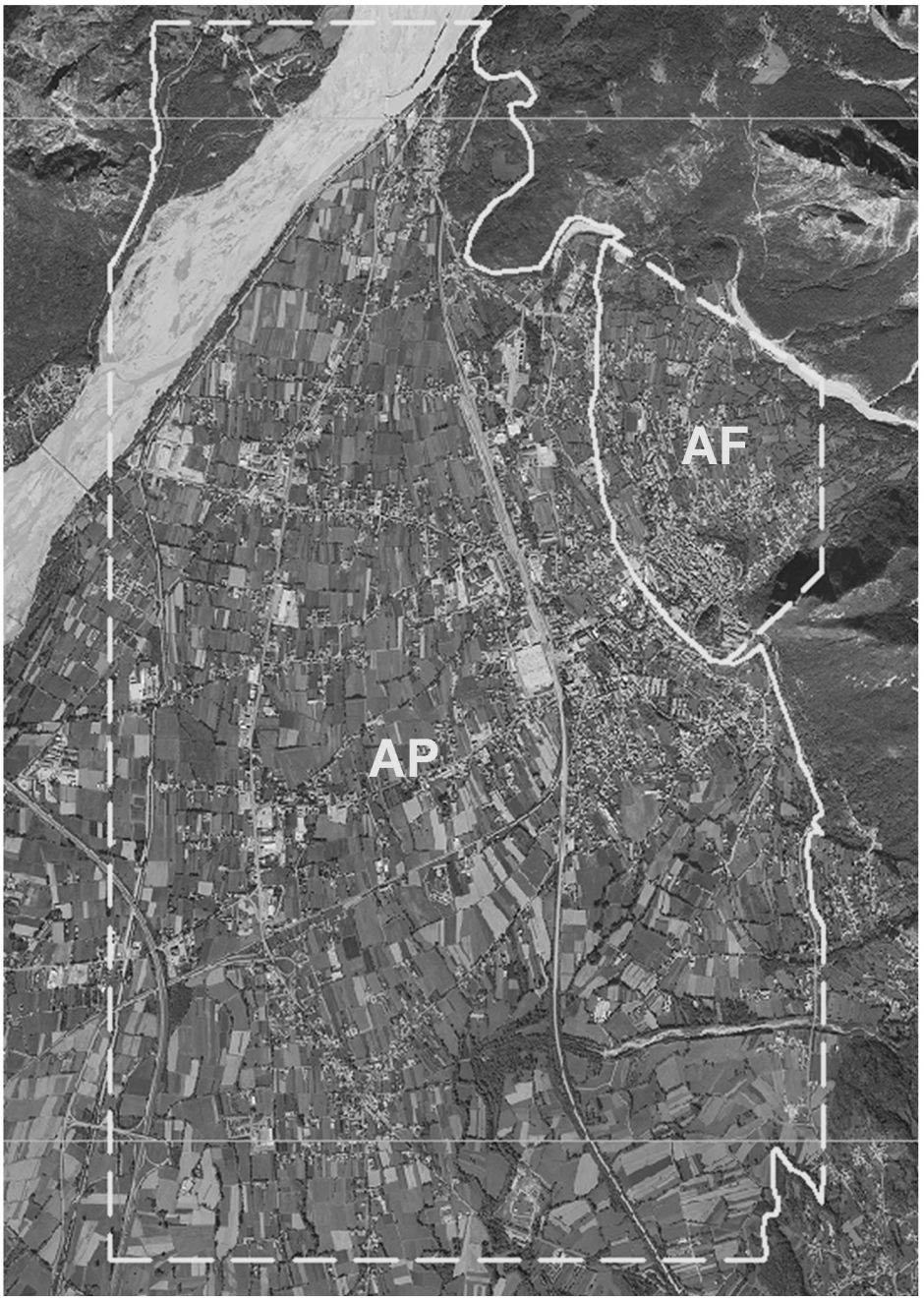

Fig. 6 - Identification of geo-morphotypes within the Gemona area.

As PGV and PGA are usually associated with motions of different frequency, the ratio v_{max}/a_{max} should be related to the frequency content of the motion (Kramer, 1996). For earthquake motions that include many frequencies, the quantity v_{max}/a_{max} can be interpreted as proportional to the period of vibration of an equivalent harmonic wave, thus providing an indication of which

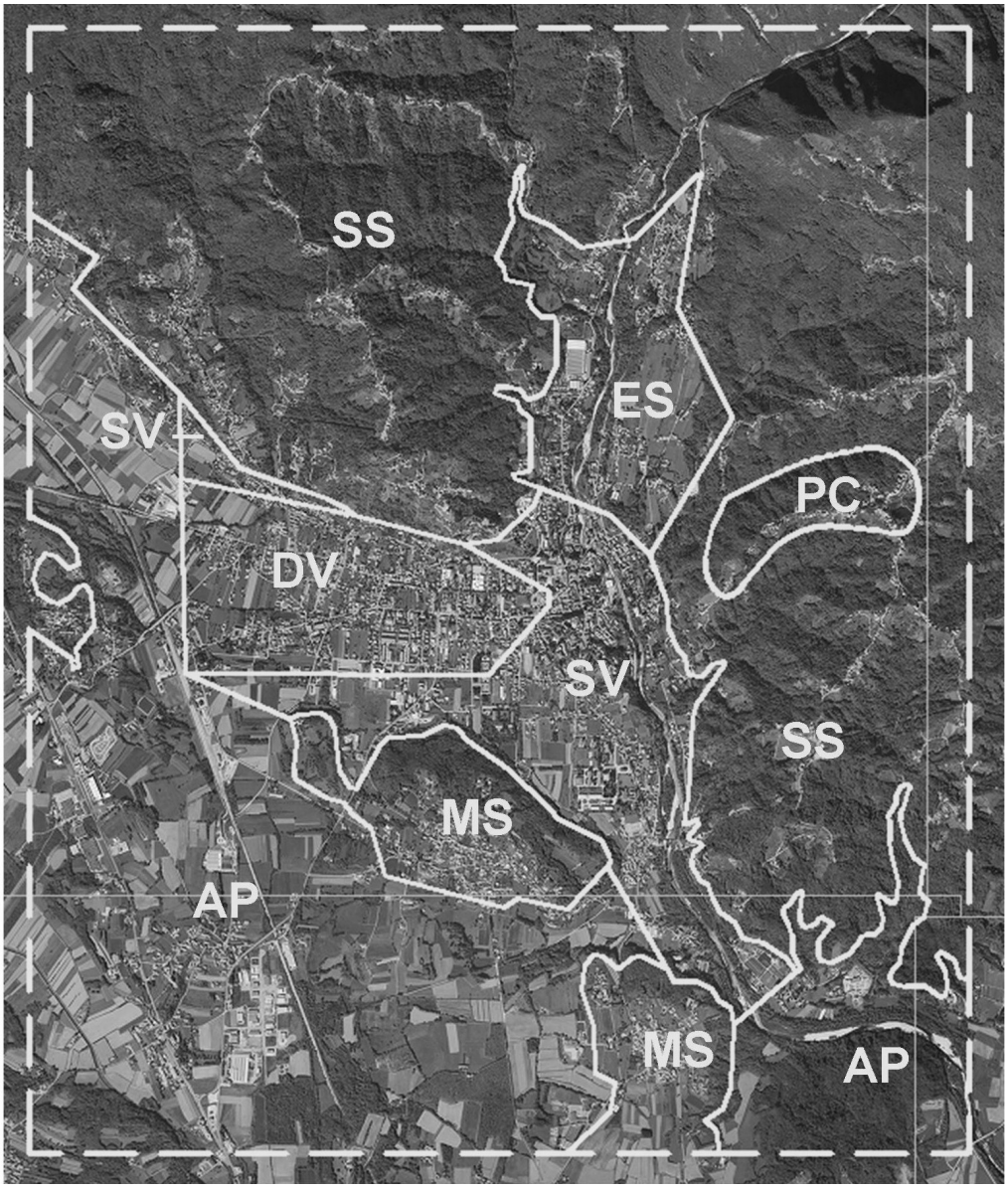

Fig. 7 - Identification of geo-morphotypes within the Tarcento area.

periods of the ground motion are most significant. Therefore, the ratio of v_{max}/a_{max} of two geo-morphotypes could be also considered as a rough measure of the amplification factor of the predominant period of ground motion.

Table 8 summarizes the results of Tables 6 and 7 reporting the computed amplification factors and indicating the characteristics of soil for each geo-morphotype analysed using the NEHRP classification.

The values found for predominant periods are in good agreement with the representative

Table 6 - Estimation of ground motion parameters by inverse Probit curves for Gemona.

GEMONA Alluvial flat plain - geo-morphotype AP							Buildings T1	366
Damage range	(%)	X_{Probit}	v_{max} (m/s)			a_{max} (m/s^2)		
			l-	o	-l	l-	o	-l
NR-D (≥G5)	26.8	4.38	0.25	0.40	1.17	2.22	2.88	3.76
RP-D (≥G4)	42.9	4.82	0.27	0.43	0.69	2.30	3.01	3.94
average estimated values and ranges of variability			0.25	0.42	1.17	2.22	2.95	3.94
GEMONA Alluvial fan - geo-morphotype AF							Buildings T1	238
Damage range	(%)	X_{Probit}	v_{max} (m/s)			a_{max} (m/s^2)		
			l-	o	-l	l-	o	-l
NR-D (≥G5)	43.1	4.83	0.35	0.64	1.77	2.67	3.78	5.36
RP-D (≥G4)	54.4	5.11	0.33	0.58	1.01	2.58	3.56	4.89
average estimated values and ranges of variability			0.33	0.61	1.77	2.58	3.67	5.36

values suggested by Seed and Idriss (1982) for different site conditions, less than 50 km from the source.

The estimated ground motion effects (Table 8) must refer to cumulative soft surface soil (where it exists) and the topographic effect. The alluvial flat plain considered as a reference geo-morphotype presents an alluvial strata of some hundreds of metres deep. The best reference geo-morphotype would be a flat rock site but that geo-morphotype is not present in the study area. Therefore, the relative amplification factors referred to a flat rock plain site have been obtained through indirect quantification considering the different amplification factors of the different classes of soil given by NEHRP (Table 9).

The relative amplification factors, ARAF, reported in Table 10, must be considered so as to include both topographic and soil-filter effects.

A rough estimation of the amplification factor for the same geo-morphotype (GMT) but with soil softer than class C could be obtained using Eq. (11).

$$ARAF(GMT\_soil\_X) = ARAF(GMT\_soil\_C) \cdot \frac{AF(soil\_X)}{AF(soil\_C)}, \tag{11}$$

where
GMT is geo-morphotype and *soil_X = D,E*
AF(soil_X), AF (soil_X) are from NEHRP, Table 9

Table 7 - Estimation of ground motion parameters by inverse Probit curves for Tarcento.

TARCENTO Alluvial flat plain - geo- morphotype AP							Buildings T1	163
Damage range	(%)	X_{Probit}	v_{max} (m/s)			a_{max} (m/s^2)		
			I-	o	-I	I-	o	-I
NR-D (≥G5)	4.2	3.27	0.08	0.12	0.38	1.17	1.48	1.86
RP-D (≥G4)	15.2	3.97	0.13	0.18	0.26	1.51	1.84	2.25
average estimated values and ranges of variability			0.08	0.15	0.38	1.17	1.66	2.25
TARCENTO Alluvial deep valley - geo-morphotype DV							Buildings T1	210
Damage range	(%)	X_{Probit}	v_{max} (m/s)			a_{max} (m/s^2)		
			I-	o	-I	I-	o	-I
NR-D (≥G5)	51.0	5.02	0.40	0.79	2.29	2.88	4.24	6.25
RP-D (≥G4)	61.4	5.29	0.37	0.69	1.29	2.77	3.94	5.62
average estimated values and ranges of variability			0.37	0.74	2.29	2.77	4.09	6.25
TARCENTO Alluvial shallow valley - geo-morphotype SV							Buildings T1	384
Damage range	(%)	X_{Probit}	v_{max} (m/s)			a_{max} (m/s^2)		
			I-	o	-I	I-	o	-I
NR-D (≥G5)	22.1	4.23	0.22	0.34	1.09	2.07	2.64	3.35
RP-D (≥G4)	40.9	4.77	0.26	0.41	0.65	2.25	2.92	3.80
average estimated values and ranges of variability			0.22	0.38	1.09	2.07	2.78	3.80
TARCENTO Edge of scarp - geo-morphotype ES							Buildings T1	88
Damage range	(%)	X_{Probit}	v_{max} (m/s)			a_{max} (m/s^2)		
			I-	o	-I	I-	o	-I
NR-D (≥G5)	42.0	4.80	0.34	0.62	2.50	2.64	3.72	5.23
RP-D (≥G4)	63.6	5.35	0.39	0.74	1.40	2.83	4.08	5.89
average estimated values and ranges of variability			0.34	0.68	2.50	2.64	3.90	5.89
TARCENTO Steep slope - geo-morphotype SS							Buildings T1	185
Damage range	(%)	X_{Probit}	v_{max} (m/s)			a_{max} (m/s^2)		
			I-	o	-I	I-	o	-I
NR-D (≥G5)	24.9	4.33	0.24	0.38	1.38	2.17	2.80	3.62
RP-D (≥G4)	47.6	4.94	0.29	0.49	0.81	2.41	3.22	4.30
average estimated values and ranges of variability			0.24	0.43	1.38	2.17	3.01	4.30
TARCENTO Moderate slope - geo-morphotype MS							Buildings T1	127
Damage range	(%)	X_{Probit}	v_{max} (m/s)			a_{max} (m/s^2)		
			I-	o	-I	I-	o	-I
NR-D (≥G5)	6.3	3.47	0.11	0.15	0.33	1.35	1.67	2.06
RP-D (≥G4)	12.6	3.86	0.11	0.16	0.23	1.41	1.73	2.12
average estimated values and ranges of variability			0.11	0.16	0.33	1.35	1.70	2.12
TARCENTO Peak or Crest - geo-morphotype PC							Buildings T1	44
Damage range	(%)	X_{Probit}	v_{max} (m/s)			a_{max} (m/s^2)		
			I-	o	-I	I-	o	-I
NR-D (≥G5)	38.6	4.71	0.32	0.57	2.10	2.55	3.52	4.87
RP-D (≥G4)	59.1	5.23	0.36	0.65	1.19	2.71	3.81	5.36
average estimated values and ranges of variability			0.32	0.61	2.10	2.55	3.67	5.36

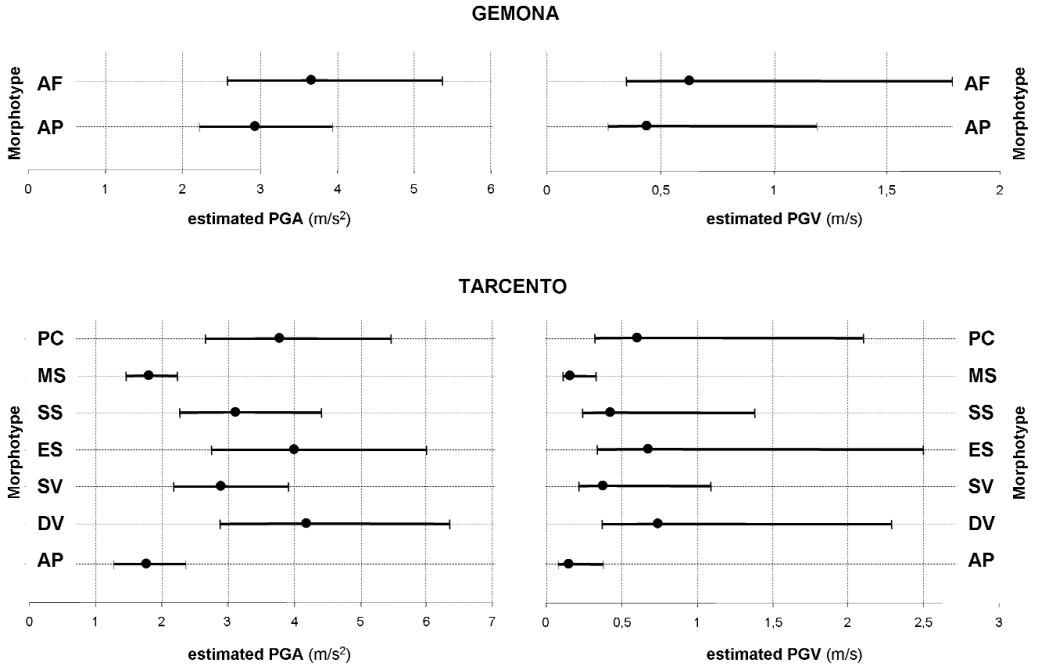

Fig. 8 - Average values and variability range of ground motion parameters estimated for the different geo-morphotypes in Gemona and Tarcento.

Table 8 - Relative amplification factors of velocity, acceleration and predominant period of ground motion referred to alluvial flat plain AP geo-morphotype.

GEMONA							
Morphotype	NEHRP class	a_{max} (m/s²)	v_{max}	v_{max}/a_{max} (s)	Average Relative Amplification Factor (AP)		
					AP(a_{max})	AP(v_{max})	AP(T_p)
AP	C	2,95	0,42	0,14	1.00	1.00	1.00
AF	C	3,67	0,61	0,17	1,24	1,45	1,17
TARCENTO							
Morphotype	NEHRP class	a_{max} (m/s²)	v_{max}	v_{max}/a_{max} (s)	Average Relative Amplification Factor (AP)		
					AP(a_{max})	AP(v_{max})	AP(T_p)
AP	C	1,66	0,15	0,09	1.00	1.00	1.00
MS	C	1,70	0,16	0,09	1,02	1,07	1,04
SV	C	2,78	0,38	0,14	1,67	2,53	1,51
SS	B	3,01	0,43	0,14	1,81	2,87	1,58
PC	B	3,67	0,61	0,17	2,21	4,07	1,84
ES	C	3,90	0,68	0,17	2,35	4,53	1,93
DV	C	4,09	0,74	0,18	2,46	4,93	2,00

Table 9 - Amplification factors defined by NEHRP for different classes of soil.

NEHRP soil class	Description	Vs (m/s)	Amplification factor AF
A	Hard rock	> 1500	0.8
B	Rock	760 - 1500	1.0
C	Very dense soil and soft rock	360 - 760	1.2
D	Stiff soil	180 - 360	1.6
E	Soft soil	<180	2.5

and ARAF(GMT_soil_C) is from Table 10.

7. Conclusions

The Probit analysis, applied to the data collected after the May 6, 1976 Friuli earthquake, has enabled us to obtain the inverse Probit curves at a regional scale. The good correlation coefficients show that these curves are a useful tool for the indirect quantification of the ground motion parameter derived from the damage recorded on buildings belonging to the same vulnerability class. Values of maximum acceleration and maximum velocity, derived in correspondence with different geomorphologic scenarios (geo-morphotypes), present in two specific areas of the region, show significant differences in the site amplification.

In particular, the comparative quantification of site effects has been referred to here as an alluvial, flat plain geo-morphotype. The larger effects of amplification were found in correspondence with deeper alluvial valleys and edges of scarps. The amplification observed was

Table 10 - Average relative amplification factors referred to rock flat plain for the different geo-morphotypes present within the areas studied.

Morphotype (NEHRP soil class)	Estimated average relative amplification factors referred to RP - Rock flat plain (B)		
	ARAF a_{max}	ARAF v_{max}	ARAF T_p
RP – Rock flat plain (B)	1.00	1.00	1.00
AP - Alluvial flat plain (C)	1,20	1,20	1,20
MS - Moderate slope (C)	1,22	1,28	1,25
AF - Alluvial fan (C)	1,49	1,74	1,40
SV - Alluvial Shallow valley (C)	2,00	3,04	1,81
SS - Steep slope (B)	2,17	3,44	1,90
PC - Peak or Crest (B)	2,65	4,88	2,21
ES - Edge of scarp (C)	2,82	5,44	2,32
DV - Alluvial depth valley (C)	2,95	5,92	2,40

of 2 or 3 times the size.

The quantitative values obtained were referred to cumulative soft soil layers (where existing) and topographic effects. Therefore, the actual amplification factors should be referred to rock site or bedrock. To achieve this, the amplification of an alluvial flat plain has been considered, taking into account the amplification given by NEHRP for that type of soil.

On the other hand, the largest scatterings of PGA and PGV estimated in Fig. 9, in correspondence to peak and crest, edge of scarp and deep valley, suggest a possible strong dependence on the direction of impinging waves with respect to the orientation of the structure. This could imply that the relevant effects cannot be ubiquitous.

Although it is important to test the results obtained by this work on a larger set of geomorphotypes, these results indicate that the geomorphologic effects can be larger than those computed with reference to the parallel plain, softer surface layers (1D and 2D models). On this point, it is interesting to observe that the new Italian seismic code (NTC08) could sensibly underestimate the site amplification factor, in particular, for typologies like a deep valley.

The results obtained can be used for a rough estimation of site effects in a preliminary microzonation or, with reference to Italy, to identify, within a municipality, an opportunity of subdividing the seismic zone into more sub-zones with different levels of site amplification factors, taking into account the different geomorphologic scenarios.

Acknowledgements. This work was made possible thanks to the completion of a project for the reconstruction of the database for the Friuli earthquake damages (Fr.E.D.) developed by the Seismic Risk Research team of the Department of Georesources and Territory of the University of Udine directed by Marcello Riuscetti and financed by the Civil Defence Department of Friuli Venezia Giulia Region (Italy). I would like to thank my colleagues of the Seismic Research team and in particular Marcello Riuscetti for his encouragement. Thanks also to Dario Slejko, Dario Albarello and Marco Mucciarelli for their useful suggestions, to Mauro Di Cecca for IT support in the geo-referencing of the Fr.E.D. database, and to Enrico Del Pin for the support in data elaborations.

REFERENCES

Carniel R., Cecotti C., Chiarandini A., Grimaz S., Picco E. and Riuscetti M.; 2001: *A definition of seismic vulnerability on a regional scale: the structural typology as a significant parameter.* Boll. Geof. Teor. Appl., **42**, 137-157.

Casarett L.J., Klaassen C.D. and Doull J.; 2001*: Dose-Response relationships.* In: Casarett and Doull's Toxicoloty: The basic sience of Poisons. 6th Ed., McGraw-Hill Professional, New York, pp. 17-24.

CCPS; 2000: *Effect models in Guidelines for chemical process quantitative risk analysis.* American Institute of Chemical Engineers, 2nd Ed., New York, pp. 244-249.

CEN (Comité Européean de Normalization); 2004: *Eurocode 8: Design provisions for earthquake resistance of structures.* Part 1.1 - General rules, seismic actions and rules for buildings, Annex A, CEN, ENV 1998-1-1, Brussels, Belgium.

Di Bucci D., Naso G., Marcucci S., Milana G. and Sanò T.; 2005: *A methodology to accout for local geology at large in the SHA approach through numerical modelling of theoretical geological sections.* Boll. Geof. Teor. Appl., **46**, 1-22.

Faccioli E.; 1991: *Seismic amplification in the presence of geological and topographic irregularities*. In: Prakash S. (ed), Proceedings of the Second International Conference on Recent Advances in Geotechnical Earthquake Engineering and Soil Dynamics, Univ. of Missouri-Rolle, **2**, pp. 1779-1797.

Faccioli E. and Cauzzi C.; 2006: *Macroseismic intensities for seismic scenarios, estimated from instrumentally based correlations*, In: 1st European Conference on Earthquake Engineering and Seismology, September 3-8, 2006, Geneva, Switzerland.

Finn W.D.; 1991: *Geotechnical engineering aspects of seismic microzonation.* In: E.E.R.I. (ed), Proceedings of the Fourth International Conference on Seismic Zonation, Oakland CA, I, pp. 199-250.

Finney D.J.; 1971: *Probit Analysis.* Cambridge University Press.

Géli L., Bard P.Y. and Jullien B.; 1988: *The effect of topography on earthquake ground motion: a review and new results.* Bull. Seism. Soc. Am., **78,** 42-63.

Giorgetti F.; 1976: *Isoseismal map of the May 6, 1976 Friuli Earthquake.* Boll. Geof. Teor. Appl., **19**, 707-714.

Grimaz S.; 1993: *Valutazione della vulnerabilità sismica di edifici in muratura appartenenti ad aggregati strutturali sulla base di analisi a posteriori.* Ingegneria Sismica, **3**, 12-22.

Grimaz S.; 2009: *Seismic damage curves of masonry buildings from Probit analysis on the data of the 1976 Friuli earthquake (NE Italy)*. Boll. Geof. Teor. Appl., **50**, 289-304.

Grimaz S., Meroni F., Petrini V., Ranù G., Tomasoni R. and Zonno G.; 1996: *Expert system for Damage assessment of buildings in seismic areas.* Cahiers du Centre Européen de Géodynamique et de Séismologie, Volume **12**, Luxembourg.

Grimaz S., Meroni F., Petrini V., Tomasoni R. and Zonno G.; 1997: *Il ruolo dei dati di danneggiamento del terremoto del Friuli nello studio di modelli di vulnerabilità sismica degli edifici in muratura.* In: Zanferrari A. and Crosilla F. (eds), La scienza e i terremoti – Forum editore, Udine, pp. 89-96.

Grünthal G.; 1998: *European Macroseismic Scale 1998 (EMS98).* Cahiers du Centre Européen de Géodynamique et de Séismologie, Volume **15**, Luxembourg.

Kramer S.L.; 1996: *Geotechnical earthquake engineering.* Prentice Hall, Upper Saddle River, 653 pp.

Laurenzano G., Priolo E. and Tondi E.; 2008: *2D numerical simulations of earthquake ground motion: examples from the Marche Region, Italy.* J. Seism. DOI 10.1007/s10950-008-9095-1.

Lees F.P.; 1996: *Injury relations.* In: Mannan S. (ed), Loss Prevention in the Process Industries. 2nd Edition, 1, Butterworth-Heinemann, Oxford, Section 9, pp. 71-76.

Martino S., Minutolo A., Paciello A., Rovelli A., Scarascia Mugnozza G. and Verrubbi V.; 2006: *Evidence of amplification effects in fault zone related to rock mass jointing.* Nat. Haz., **39**, 419-449.

Marzorati S., Luzi L., Petrini V., Meroni F. and Pergalani F.; 2003: *Detection of local site effects through the estimation of building damages.* Soil Dynam. Earthq. Eng., **23**, 497-511.

Mucciarelli M., Masi A. and Vona M..; 2003: *Quick survey of the possible causes of damage enhancement observed in San Giuliano after the 2002 Molise, Italy seismic sequence*. J. Earthq. Eng., **7**, 599-614.

Pedersen H., LeBrun B., Hatzfeld D., Campillo M. and Bard P.Y.; 1994: *Ground motion amplitude across ridges.* Bull. Seism. Soc. Am., **84**, 1786-1800.

Riuscetti M., Carniel R. and Cecotti C.; 1997: *Seismic vulnerability assessment of masonry buildings in a region of moderate seismicity.* Ann. Geof., **40**, 1405-1413.

Seed H.B. and Idriss I.M.; 1982: *Ground motions and soil liquefaction during earthquakes*. Earthquake Engineering Research Institute, Berkeley, California, 134 pp.

Vilchez J.A., Montinel H., Casal J. and Arnaldos J.; 2001: A*nalytical expression for the calculation of damage percentage using the Probit methodology.* Journal of Loss Prevention in the Process Industries, **14**, 193-197.

Wald D.J. and Allen T.I.; 2007: *Topographic slope as a proxy for seismic site conditions and amplification*. Bull. Seism. Soc. Am., **97**, 1379–1395.

Corresponding author: Stefano Grimaz
Dipartimento di Georisorse e Territorio
Università di Udine
Via Cotonificio, 114, 33100 Udine (Italy)
phone: +39 0432 558731; fax: +39 0432 558700; e-mail: stefano.grimaz@uniud.it